HHS Public Access

Author manuscript

Eur J Pharm Biopharm. Author manuscript; available in PMC 2017 December 01.

Published in final edited form as:

Eur J Pharm Biopharm. 2016 December ; 109: 224–235. doi:10.1016/j.ejpb.2016.10.015.

Topical ophthalmic formulations of indomethacin for delivery to the posterior segment ocular tissues

Sai Prachetan Balguri[1], **Goutham R Adelli**[1], and **Soumyajit Majumdar**[1,2]

[1]Department of Pharmaceutics and Drug Delivery, School of Pharmacy, The University of Mississippi, University, MS 38677

[2]Research Institute of Pharmaceutical Sciences, School of Pharmacy, The University of Mississippi, University, MS 38677

Abstract

Purpose—The objective of the present study was to formulate indomethacin (IN)-loaded solid lipid nanoparticles (SLNs) and nanostructured lipid carriers (NLCs) and to investigate their potential use in topical ocular delivery.

Methods—IN SLNs (0.1% w/v) and NLCs (0.8% w/v) were prepared, characterized and evaluated. Their *in vitro* release and flux profiles across the cornea and sclera-choroid-RPE (trans-SCR) tissues and *in vivo* ocular tissue distribution were assessed. Furthermore, chitosan chloride (CS) (mol. wt. < 200 kDa), a cationic and water-soluble penetration enhancer, was used to modify the surface of the SLNs, and its effect was investigated through *in vitro* transmembrane penetration and *in vivo* distribution tissue studies.

Results—For the IN-SLNs, IN-CS-SLNs and IN-NLCs, the particle size was 226 ± 5, 265 ± 8, and 227 ± 11 nm, respectively; the zeta potential was −22 ± 0.8, 27 ± 1.2, and −12.2 ± 2.3 mV, respectively; the polydispersity index (PDI) was 0.17, 0.30, and 0.23, respectively; and the entrapment efficiency (EE) was 81 ± 0.9, 91.5 ± 3.2 and 99.8 ± 0.2%, respectively. The surface modification of the SLNs with CS increased the ocular penetration of IN. The NLCs maintained significantly higher IN concentrations in all ocular tissues tested compared to the other formulations evaluated *in vivo*.

Conclusion—The results suggest that lipid-based particulate systems can serve as viable vehicles for ocular delivery. The NLC formulations demonstrated increased drug loading capability, entrapment and delivery to anterior and posterior segment ocular tissues.

Graphical abstract

Author for correspondence: Dr. Soumyajit Majumdar, Department of Pharmaceutics and Drug Delivery, School of Pharmacy, The University of Mississippi, 111 Faser Hall, University, MS 38677. Tel (662)-915-3793; Fax :(662)-915-1177 majumso@olemiss.edu.

Conflict of interest

The authors have declared no conflicts of interest regarding this article.

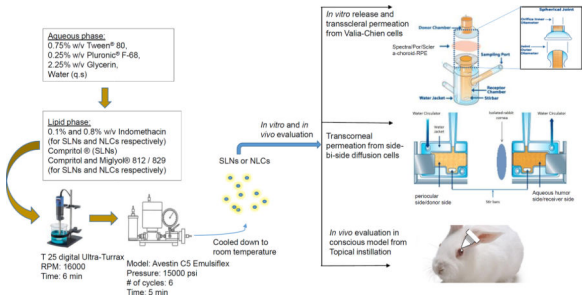

1. Introduction

Indomethacin (IN), 2-{1-[(4-chlorophenyl) carbonyl] -5-methoxy-2-methyl-1*H*-indol-3-yl} acetic acid, a topical non-steroidal anti-inflammatory drug (NSAID) is used in the treatment of the ocular inflammatory disorders such as conjunctivitis, uveitis, cystoid macular edema, and anterior segment inflammation, including post-operative pain following cataract surgery [1–3]. The compound elicits its anti-inflammatory action through the inhibition of COX-2 enzymes, which are essential for prostaglandin biosynthesis, and thus possesses analgesic and anti-pyretic properties [4]. The potential effects of prostaglandins include elevation of intraocular pressure, vasodilatation, disruption of blood ocular barriers, and leukocyte migration; hence, potent inhibition of COX-2 enzymes may provide therapeutic effects [5]. NSAIDs are employed in the treatment of diabetic retinopathy and age-related macular degeneration [6]. Formulating IN as a topical ophthalmic solution is challenging due to its poor solubility and stability [7]. Indosol, which is an aqueous solution of IN complexed in TRIS-sodium salt (tromethamine), has been widely used in ophthalmic research to treat inflammation of the anterior segment and the uvea [8]. Currently, topical ophthalmic formulations of IN are not marketed in the United States. Indocollyre® (hydro-poly(ethylene glycol) (PEG) ophthalmic) 0.1% w/v eye drops, which are commercially available in Europe, are associated with poor ocular bioavailability [9]. Conventional dosage forms and other formulation approaches have been employed to improve the intraocular penetration of IN into the posterior ocular tissues. The formulation strategies that have been tested include the application of solutions, suspensions, polymeric nanoparticles, surfactant-based systems, implants, nanomicelles, emulsions and gelling systems [10–12].

The ocular bioavailability of drugs from topical solutions is very poor, and it has been reported that less than 5–10% of the administered drug reaches the inner ocular tissues. Approaches for improving the pre-corneal residence time and transcorneal permeability characteristics could enhance intraocular bioavailability [13, 14]. In recent years, colloidal nanoparticulate systems have gained popularity as a promising ocular drug delivery platform [15]. Solid lipid nanoparticles (SLNs) and nanostructured lipid carriers (NLCs) are colloidal nanoparticulate systems designed and developed to deliver lipophilic drugs. These particulates are composed of biocompatible and biodegradable materials and are in the nanometer size range. All excipients used in these formulations are generally regarded as safe, and process scale-up is feasible. Several studies have demonstrated superior ocular bioavailability of therapeutic agents from these colloidal nanoparticulate systems, possibly because of improved retention and phagocytosis by epithelial cells. Furthermore, adsorption

of polymers, such as chitosan, on the surface of SLNs may further improve the retention of the nanoparticles on the epithelial surface and increase cellular uptake of the nanoparticles [16, 17]. Chitosan possesses favorable biological characteristics, such as biodegradability, biocompatibility and mucoadhesive properties [18, 19]. The ability of chitosan and its derivatives in ophthalmic solutions to modulate characteristics of the epithelial barrier through the transient opening of the tight junctions, which results in enhanced transmembrane absorption, has been widely reported in the literature [20–22]. In this study, chitosan was used to modify the surface characteristics of SLNs (chitosan adsorbed onto the SLN surface), and the ocular penetration of IN from the chitosan-coated SLNs was evaluated.

Varying the lipid component in the colloidal framework could also improve drug release characteristics and chemical stability. Alpha Rx developed Ocusolin™, a gentamicin loaded-SLN, is still in preclinical trials.

NLCs, however, appear to be a viable alternative to SLNs in terms of drug loading efficiency and are prepared by incorporating liquid lipids within the solid lipid structure. Depending on the ratio and concentration of the solid and liquid lipids, NLCs with different structural matrices can be obtained [23, 24].

The objective of the current study was to develop and characterize various formulations, such as SLNs, CS-SLNs and NLCs, and to evaluate the ocular delivery and disposition of IN from these topically administered formulations.

2. Materials and Methods

Compritol® 888 ATO (glyceryl behenate) was a gift from Gattefossé (Paramus, NJ, USA). Miglyol 812® and 829® were kindly supplied by Sasol, Hamburg, Germany GmbH. PROTASAN™ ultrapure Chitosan (Chitosan chloride < 200 kDa) was received from Novamatrix (Philadelphia, PA, USA). Amicon® Ultra centrifugal filter devices with regenerated cellulose membranes (molecular weight cut-off of 100 kDa), poloxamer 188, hydroxypropyl-beta-cyclodextrin (average molecular weight: 1,380; degree of substitution: 0.6), Tween®80, indomethacin, high-performance liquid chromatography (HPLC)-grade solvents, and other chemicals (analytical grade) were obtained from Fisher Scientific (Hampton, NH, USA). Whole eyes of male albino New Zealand rabbits were obtained from Pel-Freez Biologicals (Rogers, AR, USA). Male albino New Zealand rabbits were procured from Harlan Labs (Indianapolis, IN, USA).

2.1. Saturation solubility studies

Saturation solubility, as a function of pH, was studied using the standard shake-flask method. An excess amount of IN was added to screw-capped glass vials containing 200 mM phosphate buffer at different pH values, namely 5.5, 6.0, 6.5, 7.0, and 7.4, and phosphate buffer with various solubilizers, such as HPβCD, RMβCD, poloxamer 188, and Tween® 80. To achieve uniform mixing, samples were stirred at 100 rpm for 24 hrs at 25°C in a reciprocating water bath (Fisher Scientific). After 24 hrs, the samples were centrifuged (AccuSpin 17R), and the supernatant was analyzed for drug content.

2.1.1. Chromatography system for *in vitro* sample analysis—Samples were analyzed for IN content using an high performance liquid chromatography (HPLC) -UV method. The system comprised a Waters 717 plus Autosampler, a Waters 2487 Dual λ Absorbance detector, a Waters 600 controller pump, and an Agilent 3395 Integrator. A Phenomenex Luna® C_{18} 4.6 mm × 250mm column was used for the analysis. The mobile phase used was methanol, water, and orthophosphoric acid (70:29.05:0.05). The detection wavelength λ^{max} for IN was 270 nm. The flow rate was set to 1mL/min during the analysis.

2.2. Formulations

IN-TSOL, IN-SOL and IN-CS-SOL formulations—IN-TSOL was prepared by dissolving 0.1% w/v IN in 1% w/v Tween® 80 solution, which was used to investigate the release characteristics compared to the test formulations and to evaluate barrier resistance. Additionally, IN-SOL was prepared by dissolving IN (0.1% w/v final concentration) in an aqueous solution containing Tween®80 (1% w/v) and propylene glycol (29.3% w/v). Sodium hydroxide (1N) was added in small increments to adjust the pH. IN-CS-SOL was prepared by adding chitosan chloride (CS; 0.1% w/v final concentration) to IN-SOL. The pH of the final formulations was maintained at 6.8 because Indocollyre®, a formulation marketed in Europe, is at this pH.

IN-HPβCD and IN-CS- HPβCD solution formulations—IN-HPβCD formulation was prepared by dissolving IN (0.1% w/v) in 2.5% w/v HPβCD solution prepared in isotonic phosphate-buffered saline (IPBS; pH 6.8). IN-CS-HPβCD was prepared by the addition of 0.1% w/v CS to the IN-HPβCD formulation. The final pH of the formulations was adjusted to 6.8.

Indomethacin solid lipid nanoparticles (IN-SLN) and IN-SLN-HPβCD formulations—The solubility of IN in a wide variety of lipids was visually evaluated to select suitable lipid excipients for formulating the SLNs/NLCs. IN-loaded SLNs were prepared based on a hot homogenization method. Solid lipid, namely Compritol® 888 ATO, was melted, and IN (5% w/w with respect to the lipid) was dissolved therein to obtain a clear lipid phase. Simultaneously, an aqueous phase prepared using the surfactants poloxamer 188 (0.25% w/v) and Tween® 80 (0.75% w/v) and glycerin (2.25% w/v) in bidistilled water, was heated. The hot aqueous phase was added to the melted lipid phase while stirring, and the premix was then subjected to emulsification at 16,000 rpm for 6 min using a T 25 digital Ultra-Turrax. The pre-emulsion obtained was homogenized under high pressure, using previously optimized process parameters (15–20 K psi; 6 cycles; 6 min), using a thermostated Emulsiflex C5 (Avestin) resulting in the formation of a hot emulsion dispersion [9]. The sample cylinder was preheated and maintained at 80±2°C during the entire process using an electrical cord harness that was wrapped and securely fastened to the sample cylinder and connected to an external thermostat. The hot emulsion obtained was slowly cooled to room temperature to form the IN-SLNs. The final concentrations of Compritol® 888 ATO and IN in the formulation were kept constant at 2% w/v and 0.1% w/v, respectively.

Additionally, a variation of the IN-SLN formulation was prepared wherein 2.5% w/v HPβCD (final concentration) was added to the aqueous phase described above prior to the preparation of the SLNs. The pH of the resulting formulations was adjusted to 6.8 using NaOH (1N).

Indomethacin nanostructured lipid carriers (IN-NLCs)—The NLCs contained both solid (Compritol 888® ATO) and liquid lipids (Miglyol® 812 or 829), unlike the SLNs, which contained only solid lipids. The total amount of lipid employed in the NLCs was 4 and 8% w/v, of which Compritol 888® ATO constituted 60% and Miglyol® 812 or 829 made up the remaining 40% of the lipids. The concentration of surfactants (Tween 80® and poloxamer 188) and propylene glycol in the NLC formulations were maintained identical to that in the SLNs. Drug loading in all NLC formulations was kept constant at 0.8% w/v. The prepared formulations were then characterized and evaluated with respect to *in vitro* release and transcorneal permeation and *in vivo* ocular tissue levels.

Chitosan-coated IN solid lipid nanoparticles (IN-CS-SLNs)—CS (mol. wt. < 200 kDa) was used for surface modification of the SLNs. CS (0.1% w/v) was incorporated into the aqueous phase prior to preparation of the SLNs, as described above (*in vitro* studies). CS at a concentration of 0.25% w/v was used in the SLNs for the *in vivo* experiments. Surface modification of the CS-coated formulations was confirmed through zeta potential measurements.

2.3. Particle size, polydispersity index (PDI) and zeta potential measurements

The hydrodynamic radius and the PDI of the SLN dispersion, the IN-CS-SLNs and the IN-NLCs were determined by photon correlation spectroscopy using a Zetasizer Nano ZS Zen3600 (Malvern Instruments, Inc.) at 25°C and with 173° backscatter detection in disposable folded capillary clear cells. The measurements were obtained using a helium-neon laser of 633 nm, and the particle size analysis data were evaluated based on the volume distribution.

Zeta potentials were measured at 25°C in folded capillary cells using the same instrument. To measure the particle size distribution and zeta potential, the SLN samples were diluted (1:500) with water. Bidistilled and 0.2-μM filtered waters were used for these measurements and were performed in triplicate.

2.4. Assay and entrapment efficiency (EE)

The lipid in the IN-SLN dispersion, the IN-CS-SLNs and the IN-NLCs was precipitated using 190-proof alcohol (“over proof’’), or 95% alcohol by volume (“ABV”), and the drug content in the supernatant after centrifugation (13,000 rpm for 20min), as such or after further dilution with 190-proof alcohol, was measured using an HPLC system.

The percentages of IN entrapped (% EE) in the IN-SLNs and IN-NLCs were determined by measuring the concentration of free drug in the aqueous phase of an undiluted formulation. The EE was evaluated by an ultrafiltration technique with a 100-kDa centrifugal filter device that included a regenerated cellulose membrane (Amicon Ultra). A 500- μL aliquot of the

corresponding formulation was added to the sample reservoir and centrifuged at 5,000 rpm for 10min. The filtrate was then further diluted with 190-proof alcohol and analyzed for drug content using HPLC-UV (Section 2.1). The % EE was calculated using Eq. (1).

$$\%\mathrm{EE}=\left[\frac{\mathrm{wi}-\mathrm{wf}}{\mathrm{wi}}\right]\times 100 \quad (1)$$

where W_i is the total drug content, and W_f is the amount of free drug in the aqueous phase.

2.5. Terminal moist-heat sterilization and stability assessment of IN formulations

Two batches each of the optimized IN lipid-based formulations, namely the IN-SLNs, the IN-CS-SLNs and the IN-NLCs, were prepared and subjected to moist-heat sterilization (121°C for 15 min at 15 psi) in appropriately labelled glass vials using a thermo-controlled autoclave (AMSCO® Scientific Model SI-120). Following autoclaving, the sterilized samples were evaluated in terms of their physical appearance, color, particle size and physicochemical characteristics compared to un-sterilized reference formulations that were maintained at room temperature.

Additionally, three batches of IN-SLNs, IN-CS-SLNs and IN-NLCs were evaluated for their physical and chemical stability upon storage for a period of 3 months at 40°C/60% RH, 25°C/75% RH and 4°C. The particle size, PDI, zeta potential, EE and drug content were evaluated, as described in Sections 2.1 and 2.3.

2.6. Fourier transform infrared spectroscopy (FTIR)

The infrared spectra (IR) of the SLN and NLC formulations were obtained using Cary 660 series FTIR (Agilent Technologies) and MIRacle ATR (attenuated total reflectance) systems. The ratios of drug and lipids used in this set of studies were similar to the weight ratios in the IN lipid formulations.

2.7. *In vitro* release studies

In vitro release profiles of IN from the respective formulations, such as the IN-Tween® 80 solution (IN-TSOL), the IN-SLNs and the IN-NLCs (F-1 and F-2), were evaluated using Valia-Chien cells (PermeGear, Inc.). Spectra/por® dialysis membranes (3.5K MWCO) were mounted on diffusion cell chambers and securely fastened with air tight clamps between the donor and receptor chambers through which the transport or release kinetics were being studied. The temperature of the cells was maintained at 34°C using a circulating water bath. Five milliliters of isotonic phosphate buffer (IPBS) (pH 7.4) containing 2.5% w/v RMβCD was used as the receptor media during the course of the study (6 hrs). Five hundred microliters of formulation was added to the donor chamber. The, 600-μL aliquots were withdrawn from the receiver chamber at predetermined time points and replaced with an equal volume of the 2.5% w/v RMβCD in IPBS (pH 7.4) solution. The donor concentration was maintained at 0.1% w/v in all the formulations. The samples taken were analyzed using a HPLC-UV system, as described in Section 2.1.

2.8. *In vitro* corneal permeation studies

Corneas excised from whole eyes, obtained from Pel-Freez Biologicals, were used for the determination of *in vitro* transcorneal permeability. The whole eyes were shipped overnight in Hanks' balanced salt solution over wet ice and were used immediately upon receipt. The corneas were excised with some scleral portion adhering to help secure the membrane between the diffusion half-cells during the course of the transport study. After excision, the corneas were washed with the IPBS (pH 7.4) and mounted on side-by-side diffusion half-cells (Perme Gear, Inc®) with the epithelial side facing the donor chamber. The temperature of the half-cells was maintained at 34°C via a circulating water bath. The IN contents in the IN-SLN, IN-CS-SLN and IN-NLC formulations were 0.1% w/v, 0.1% w/v and 0.8% w/v, respectively. Three milliliters of the optimized IN-SLNs, IN-CS-SLNs or IN-NLCs was added to the donor chamber after adjusting the pH to 6.8. The donor IN concentration was maintained at 0.1% w/v in the SLN formulation and 0.8% w/v in the NLC formulation. The receiver chamber medium consisted of 3.2 mL RMβCD (2.5% w/v) in IPBS solution for all the transport studies. The difference in the volume of liquid between the two half-cells (3 mL on one side and 3.2 mL on the other) creates a pressure difference across the corneal membrane. Due to this difference in hydrostatic pressure, the cornea bulges out, the circumference of the corneal/scleral limbus is clamped together by the two half-cells toward the half-cell with less volume, thus mimicking the natural curvature of the cornea [25–28]. The contents of both chambers were stirred continuously with a magnetic stirrer. Aliquots (600 μL) were withdrawn from the receiver chamber at predetermined time points up to 3 hrs and replaced with an equal volume of 2.5% w/v RMβCD in IPBS. The samples were stored at −80°C until further analysis of IN using the chromatography system described in Section 2.1. Additionally, the transcorneal permeabilities of IN from the IN-SOL formulation (control) and IN-HPβCD in the presence of CS as a penetration enhancer were also determined.

2.9. Trans-SCR permeability studies of IN formulations

The scleral tissue with the retinal pigmental epithelium and choroid layers excised from whole eyes, obtained from Pel-Freez Biologicals, were used to determine the *in vitro* trans-SCR (sclera-choroidal RPE) permeability of IN from the formulations. After excision, the scleral membranes were washed with IPBS (pH 7.4) and mounted on Valia-Chien cells (Perme Gear, Inc®). The scleral tissues were mounted as an inverted cup onto diffusion cells between the donor and receptor chamber and fastened securely with air tight clamps such that the scleral membrane was exposed to the donor compartment (episcleral side) and the RPE-choroidal tissues were in contact with the receptor compartment (vitreous body side). Five milliliters of 2.5% w/v RMβCD solution prepared in IPBS (pH 7.4) was used as the media in the receiver chamber during the course of the study for 2.5 hrs. Five hundred microliters of IN-SOL, IN-HPβCD, IN-SLNs (pH 6.8 and 7.4), and IN-SLNs+HPβCD were added to the donor chambers, and the concentration was maintained at 0.1% w/v. Aliquots (600 μL) were withdrawn from the receiver chamber at predetermined time points (15, 30, 45, 60, 90, 120 and 150 min) and replaced with an equal volume of receiver medium. The samples taken were analyzed using the HPLC-UV system as discussed in Section 2.1.

2.10. *In vivo* bioavailability studies

In vivo bioavailability of IN was determined in Male New Zealand White albino Rabbits, weighing between 2–2.5 kg, procured from Harlan Labs. All the animal studies conformed to the tenets of the Association for Research in Vision and Ophthalmology statement on the use of animals in ophthalmic vision and research and the University of Mississippi Institutional Animal Care and Use Committee approved protocols. Rabbits were anesthetized using a combination of ketamine (35 mg/kg) and xylazine (3.5 mg/kg) injected intramuscularly and were maintained under anesthesia throughout the experiment. The IN formulations, namely the IN-SOL, IN-HPβCD, and IN-SLNs, were evaluated *in vivo*. All the above IN topical formulations (100 μL) were given as two doses (50 μL), 30 min apart, (T-30 min and 0 min) to reduce precorneal loss. Additionally, the IN-CS-SOL, IN-SLNs, IN-CS-SLNs (n=6) and IN-NLCs were administered to conscious rabbits to delineate the effects of anesthesia on the ocular bioavailability of IN. CS was used at a concentration of 0.25% w/v (*in vivo)*. Two hours post-topical application, the rabbits were euthanized with an overdose of pentobarbital injected through a marginal ear vein. The eyes were washed thoroughly with ice-cold IPBS and were immediately enucleated. All the intraocular tissues were separated and stored at −80°C, and further analysis was carried out using the HPLC-UV system (Section 2.1). All experiments were performed in triplicate.

Biosample preparation for the determination of IN content in ocular tissue homogenates—The *in vitro* analytical HPLC-UV method described above was employed for sample analysis following method validation. A protein precipitation technique was employed to determine the amount of IN in the ocular tissue homogenates. Briefly, tissues including the cornea, sclera, iris-ciliary (IC), and retina-choroid (RC) were cut into small pieces, and a mixture of ice-cold acetonitrile and 0.1% v/v formic acid was added (1 mL) to precipitate proteins from each individual tissue. The supernatant was then collected via centrifugation for 1 hr at 13000 rpm prior to the analysis. The aqueous humor (AH) (200 μL) and vitreous humor (VH) (500 μL) were precipitated by adding an ice-cold mixture of acetonitrile and formic acid, 200 μL of each for the AH and 500 μL of each for the VH corresponding to a ratio of 1:1. Quantification of IN was performed using standard calibration curves constructed from various ocular tissues, such as the cornea (20–500 ng), the sclera (20–500 ng), the AH (10–200 ng), the VH (10–200 ng), the IC (10–200 ng), and the RPE (10–200 ng). All the standard curves had a coefficient of determination $r^2 \geq 0.96$. The recovery of IN was evaluated by spiking the drug in pure AH and VH and comparing the expected IN concentration with the standard concentration. Recovery values were determined for AH (93.1) and VH (91.5). Interference was not observed from co-eluted protein residues with respect to IN peaks in any of the tissues. The limit of detection (LOD) for various ocular tissues was determined and corresponded to 10 ng for AH, 10 ng or VH, 5 ng for the cornea, 5 ng for the sclera, 10 ng for the RPE, and 10 ng for the IC.

2.11. Data analysis

The steady-state flux (SSF) for transcorneal and trans-SCR experiments was calculated by dividing the rate of transport by the surface area. The slope of the cumulative amount of IN transported versus time plot was used to obtain the rate of IN transport across the excised rabbit cornea. The flux was calculated using the Eq. (2).

$$\text{Flux(J)}=(\text{dM}/\text{dt})/\text{A} \quad (2)$$

where M is the cumulative amount of drug transported, and A is the surface area of the corneal membrane (0.636 cm^2) exposed to the permeant (drug).

The transcorneal permeability was determined by normalizing the SSF to the donor concentration, C_d, according to Eq. (3).

$$\text{Permeability(Papp)}=\text{Flux}/\text{Cd} \quad (3)$$

2.12. Statistical analysis

One-way-ANOVA coupled with a post hoc test was employed to analyze the differences between groups (*in vivo*). The difference in data obtained were considered statistically significant at level of $p<0.05$.

3. Results

3.1. Morphometrical and physico-chemical characteristics

The particle size, zeta potential, PDI and EE of IN-SLN, the IN-CS-SLNs and the IN-NLCs were observed to be 226 ± 5, 265 ± 8, and 227 ± 11 nm; −22 ± 0.8, 27 ± 1.2, and −12.2 ± 2.3 mV; 0.17, 0.30, and 0.23; and 81 ± 0.9, 91.5 ± 3.2 and 99.8 ± 0.2%, respectively. The quantitative compositions of the various IN formulations are presented in Table 1. The particle size of the IN-NLCs increased as the total lipid content increased, and IN-NLC-F1 appears to be a promising formulation, exhibiting a lower hydrodynamic radius and better physico-chemical characteristics compared to the other formulations (Table 2).

3.2. Solubility of IN in the presence of cyclodextrins and surfactants

Cyclodextrins and surfactants are frequently employed as solubilizers in topical ophthalmic formulations. The solubilities of IN in 0.25 and 0.5% w/v poloxamer 188 at pH 7.4 were measured as 251.8 ± 78 and 657 ± 127 μg. The solubility of IN in 0.5% w/v Tween® 80 at pH 7.4 was determined to be 1055 ± 106 μg. The solubility profiles of IN in 5% w/v HPβCD and RMβCD were found to be similar. However, the solubility of IN is highly pH-dependent and tends to be predominantly solubilized at high pH (Figure 1).

3.3. Stability, moist-heat sterilization and FTIR studies

IN-CS-SLNs and IN-NLCs exhibited good stability when compared to the IN-SLN formulation. The particle size of the IN-SLN formulation after storage for 90 days at 40°C was increased by 65%, whereas the IN-CS-SLNs and IN-NLCs displayed a 15–20% increase in particle size (Figure 2). Additionally, the EE of the SLN formulations decreased by 12% compared to the IN-CS-SLNs (6%) and IN-NLCs (5%) (Figure 3A). The zeta potential and PDI of the IN formulations were not changed significantly under the storage conditions tested here (Figure 3B and 3C). Figure 4 shows the effect of sterilization on the

physicochemical characteristics of the IN lipid-based formulations. No significant differences were observed post-sterilization. The particle size of the IN-CS-SLNs and IN-NLC formulations slightly increased compared to the IN-SLNs following autoclaving. Additionally, the FTIR spectra revealed a slight drug-excipient interaction in the lipid formulations (Figure 5).

3.4. *In vitro* release studies

Based on the solubility profile of IN in different solubilizing agents, RMβCD in IPBS at pH 7.4 was chosen as the receptor media for the *in vitro* release and transcorneal permeability experiments. The *in vitro* releases of IN from the IN-TSOL, the IN-SLNs, the F-1IN-NLCs, and the F-2 IN-NLCs were observed to be 81.6 ± 2.1 μg, 18.7 ± 0.9 μg, 31.8 ± 3.9 μg, and 23.3 ± 3.1 μg within the time period tested (6 hrs). The *in vitro* release of IN from these formulations is depicted in Figure 6.

3.5. Transcorneal permeability studies

The transmembrane permeabilities of IN from the IN-SLNs, the F-1IN-NLCs, and the F-2 IN-NLCs were observed to be $1.93 \pm 0.17 \times 10^{-5}$, $1.34 \pm 0.13 \times 10^{-5}$, and $1.2 \pm 0.1 \times 10^{-5}$ cm/s, respectively. The transcorneal flux of IN was increased by two-fold when CS was used as a permeation enhancer in the SLN formulation. Moreover, the effect of including CS as a penetration enhancer in the solution formulations, namely in IN-SOL and IN-HPβCD, was also investigated. CS significantly enhanced the transcorneal flux of IN by ~3.5 and ~2-fold for the IN-SOL and IN-HPβCD formulations, respectively (Figure 7).

3.6. Trans-sclera-choroid-RPE (SCR) permeability studies

Trans-SCR permeability experiments were carried out to assess the scleral penetration capability of IN from the formulations compared to the corneal absorption route. The trans-SCR permeability of IN-HPβCD was markedly higher compared to IN-SOL. The trans-SCR permeabilities of the SLN increased in the order of IN-SLNs (pH 6.8) < IN-SLNs (pH 7.4) < IN-SLNs + HPβCD (pH 6.8). The SLNs in combination with HPβCD demonstrated a higher trans-SCR permeability than the SLN formulation alone (Figure 8).

3.7. *In vivo* bioavailability studies

Based on the transcorneal and trans-SCR data obtained, the IN formulations were investigated for their ocular bioavailability and disposition of IN 2 hrs post-topical administration in anesthetized and conscious rabbits. The IN-SOL formulation could not deliver the drug to the posterior ocular tissues. However, the IN-SOL formulation was able to achieve drug levels in the anterior segments of the eye, including 463.5 ± 15 ng/g in the cornea and 224 ± 8.6 ng/g in the scleral tissues. CS as a penetration enhancer further improved the ocular bioavailability of IN-SOL. Significant drug levels were attained from the IN-HPβCD formulation in most of the ocular tissues tested, namely in the cornea (3267.3 ± 1867.6 ng/g), the sclera (575.7 ± 433.5 ng/g), the AH (877.4 ± 492.5 ng/g), the RC (94.4 ± 79.9 ng/g) and the IC (1203.9 ± 547 ng/g). Significantly higher levels of IN were observed in the posterior segments of the eye for the use of the SLN formulation compared to the IN-SOL and IN-HPβCD formulations. The formulation of SLNs in combination with

0.25% w/v CS achieved higher levels of IN in conscious rabbits (n=6). The NLC formulations, however, were the most effective in terms of drug loading and ocular IN levels. The ocular tissue IN concentrations obtained from the above formulations are shown in Figures 9 and 10.

4. Discussion

The objective of the current work was to develop IN-loaded lipid-based nanoparticles and to investigate the *in vitro* corneal permeation and *in vivo* ocular disposition of IN from these formulations. Most NSAIDs are inherently weak acidic drugs with poor corneal penetration due to their ionization at lacrimal pH. Lowering the pH of these formulations increases corneal penetration but also increases potential irritation. Additionally, it has been reported that due to the anionic nature of NSAIDs, they are incompatible with preservatives such as benzalkonium chloride and could form insoluble complexes [29–31]. IN (pKa of 4.5) exhibits pH-dependent solubility, which increases as a function of higher pH (acidic to neutral/alkaline: 1.5 μg/mL at pH 1.2 and 105.2 μg/mL at pH 7.4). IN displayed a solubility of 0.64 ± 0.02 mg/mL in phosphate buffer at pH 7.0, which is consistent with previously reported data [32, 33]. Additionally, the solubility of IN was increased by ~5 and ~6-fold with 5% w/v HPβCD and RMβCD in phosphate buffer at pH 7.0.

SLNs and NLCs are colloidal nanoparticulate dispersions that can be administered topically in the form of eye drops. A major advantage of the nanoparticulate systems is their uptake by epithelial cells, which allows for greater penetration into the surface layers [34–36]. Moreover, the small size, biocompatibility and mucoadhesive properties of SLNs improve their interactions and prolong the pre-ocular residence time of drugs, thus enhancing drug bioavailability [37, 38]. The literature suggests that surface modification of SLNs by coating with hydrophilic agents such as poly (ethylene) glycol derivatives (PEGs) or chitosan can further improve ocular penetration, mainly due to enhancing interactions with the ocular mucosa and increasing cellular uptake and internalization [39, 40]. Additionally, previous reports have demonstrated the ability of chitosan nanoparticles to produce a sharp, reversible decrease in the transepithelial electrical resistance (TEER) and to improve the permeability of model macromolecules [41]. The mechanism of mucoadhesion is possibly through the electrostatic interaction between the positively charged amino groups of chitosan and the negatively charged sialic acid residues of ocular mucosa [42].

The corneal route is a major absorption pathway for topically administered medications [43]. Compared to other formulations, IN-SLNs demonstrated higher transcorneal permeability, which may be ascribed to endocytosis or transcytosis uptake mechanisms [44, 45]. The *in vitro* transcorneal permeability of IN from the NLC formulations was comparatively lower than that of the SLNs, probably because of higher entrapment in the oily phase and thus lower partitioning into the membrane. Reports have suggested that chitosans with a moderate degree of deacetylation (65–80%) and a relatively high molecular weight (170–200 kDa) is required for the exertion of optimal transepithelial penetration and low toxicity [46–48]. The *in vitro* transcorneal flux of IN from the IN-SOL, IN-HPβCD, and IN-SLN formulations increased by 3.5-fold, 2-fold and 2-fold, respectively, in the presence of CS, which is consistent with previous reports.

Numerous reports have demonstrated that sclera is more permeable to hydrophilic than to lipophilic molecules and approximately 10 times more permeable than the cornea [49, 50]. Based on trans-scleral transport studies, the higher permeability across several static layers of ocular tissues (sclera, Bruch's membrane-choroid, RPE, and neural retina) demonstrates the diffusional ability of drugs to the back of the eye through the conjunctival-scleral pathway [51, 52]. To investigate drug delivery to the posterior ocular segments, scleral diffusion of IN was assessed in trans-SCR experiments. The higher observed trans-scleral permeability of IN from the SLNs compared to the IN-SOL and IN-HPβCD formulations demonstrated that lipid carriers could enhance accumulation in scleral tissue, prolonging the ocular residence time *in vivo*. The increased permeability of IN from SLNs with HPβCD in external aqueous phase could be due to the complexation effect of cyclodextrin with the free drug. The trans-scleral permeability of SLNs at pH 7.4 ($2.99 \pm 0.1 \times 10^{-5}$ cm/s) was considerably higher than that of the SLNs at pH 6.8 ($2.13 \pm 0.3 \times 10^{-5}$ cm/s), which is likely due to an increase in the ionized fraction of IN at pH 7.4. Castelli et al. [53] fabricated SLNs and NLCs of IN and characterized the formulations with respect to drug distribution and entrapment efficiencies in the lipid matrices. However, the loaded drug in the SLNs and NLCs of IN was maintained at 2 and 1.5% w/w with respect to the total lipid, whereas in the present study, drug loading of IN in the SLNs and NLCs was achieved at 5 and 20% w/w, respectively. The IN lipid formulations demonstrated higher drug loading and entrapment efficiencies at lower lipid contents compared to Castelli's formulations. Bucolo et al. [54] investigated the ocular pharmacokinetics of IN following a multiple dosing treatment regime (30 μL/eye; four times in 8 hrs) of 0.5% IN + hydroxypropylmethylcellulose, IN-HPMC and Indocollyre® eye drops in conscious rabbits. The drug levels in the AH, RC and VH obtained 2 hrs post-topical administration of IN-HPMC and Indocollyre® solution were 360 ± 40 and 100 ng/mL, 65 and 20 ng/g, and 7± 2 and 5 ± 2 ng/mL, respectively. Campos et al. [42] studied the ocular distribution of chitosan-fluorescein nanoparticles (0.25% w/v, dose: 100 μL, 250 μg) and their interaction with the corneal and conjunctival epithelia in conscious rabbits. The drug levels in the cornea and conjunctiva 2 hrs post-topical application were 760 ± 60 and 1000 ± 150 ng/g, respectively. In another study, Klang et al. [55] formulated positively charged submicron emulsions (0.1% w/v) and compared the formulation with Indocollyre®. The drug concentrations obtained in the cornea and conjunctiva 1 hr after topical instillation of 50 μL of the test formulation were nearly 40 and 30% lower, respectively, compared to the marketed formulation. The drug concentrations obtained in the AH and sclera-retina were found to be 75 ± 38 ng/mL and 800 ± 310 ng/g (submicron emulsion) vs 110 ± 50 ng/mL and 450 ± 200 ng/g (Indocollyre®), respectively. Yamaguchi [56] et al. investigated ocular tissue IN concentrations upon use of chitosan-coated emulsion (0.1% w/v) formulations 1 hr post-topical instillation (50 μL) in both eyes of anesthetized male Japanese albino rabbits. The drug levels attained were predominantly in the cornea (3596±425 ng/g), aqueous humor (434±90 ng/mL) and conjunctiva (668 ± 188 ng/g). In another study, an IN (0.1% w/v) ophthalmic solution was prepared using Poloxamer® 407 (10% w/w) and compared with an Indocollyre® formulation in terms of AH concentration 2 hr after a multiple post-topical administration regime of 150 μL (6 × 25 μL at 90 sec intervals). The IN concentration in the AH was enhanced by ~2-fold compared to the use of Indocollyre® [7].

In comparison to all the ocular tissue levels obtained with the above-discussed formulations, the IN-CS-SLNs delivered significantly higher levels of IN to the anterior and posterior segment ocular tissues, which could be attributed to mucoadhesive and epithelial barrier-modulating properties of chitosan. Compared to IN-SOL without CS, the incorporation of CS in the IN-SOL formulation improved penetration of IN into the AH and IC bodies, but retinal tissue IN levels remained below the detection limit. The addition of viscosity modifiers, such as hydroxypropyl methylcellulose, in the IN-CS-SOL formulation may further prolong the precorneal residence and thus increase ocular drug levels. IN concentrations were reduced by ~4- to 5-fold in conscious animals compared to the anesthetized model, delineating the effects of anesthesia on ocular pharmacokinetics. In comparison, at higher doses (0.8% w/v; 8-fold dose) the IN-NLCs delivered ~4- to 5-fold higher concentrations than the IN-CS-SLNs, which could be due to higher drug loading, EE and pre-ocular retention of IN for the use of the NLC formulation. NLCs are superior to SLNs in terms of higher drug loading, higher EE, improved storage stability and less drug expulsion during storage.

The effect of storage conditions and sterilization on the morphometrical and physico-chemical characteristics of IN formulations are shown in Figures 2–4. There was initially no significant difference in particle size, zeta potential, or PDI between the SLNs and NLCs, but as the time progressed, the IN-NLC and IN-CS-SLN formulations were found to be more stable than the IN-SLNs. The EE of the formulations decreased slightly as the storage time increased, although the change was not statistically significant (Figure 3A). Sterilization trials suggested that the IN lipid-based formulations were autoclavable (Figure 4). A qualitative FTIR spectral analysis was employed to investigate any interactions and/or incompatibility among the lipid, drug and other excipients. The FTIR spectra of the physical mixture indicated slight molecular interactions between the drug and Compritol. The characteristic peaks of IN at 1,711 cm^{-1} (carbonyl stretching-acid group), 1,221 cm^{-1} (asymmetric aromatic O–C stretching) and 1,086 cm^{-1} (symmetric aromatic O–H stretching) are masked in the formulations possibly due to the amorphous transition and entrapment of IN in the lipid matrices. In conclusion, the results obtained here indicate that lipid-based systems can dramatically improve the transcorneal permeability and retention characteristics of IN compared to conventional formulations *in vivo*. Thus, colloidal frameworks could be exploited to enhance ocular bioavailability significantly, including back-of-the-eye ocular tissues.

5. Conclusion

Targeting NSAIDs to the posterior segment of the eye via a topical route is a challenging task due to formulation constraints and the anatomical, physiological and efflux barriers present in ocular tissues. IN-loaded NLC formulations displayed higher drug-loading capabilities and entrapment efficiencies, which resulted in higher IN levels in the ocular tissues. The IN-CS-SLNs demonstrated superior trans-membrane IN permeation characteristics compared to the IN SLNs, confirming the penetration-enhancing properties of chitosan. It is worth noting that the IN-CS-SLNs, containing a tenth of the loaded drug of the IN-NLCs, induced IN concentrations in the inner ocular tissues (the AH, IC and RPE-choroid) that were 3- to 4-fold lower than those obtained for IN-NLCs. The corneal and

scleral IN concentrations achieved using the IN-NLCs were significantly higher, indicating the effect of the increased drug loading in the formulation. Thus, both the IN-CS-SLNs and IN-NLCs are viable platforms for the delivery of IN to the posterior segment ocular tissues.

Acknowledgments

This work was supported by grants 1R01EY025365-01 and P20 GM104932 from the National Center For Research Resources. The content is solely the responsibility of the authors and does not necessarily represent the official views of the National Center for Research Resources or the National Institutes of Health.

Abbreviations

IN	Indomethacin
IN-TSOL	IN in Tween® 80 solution
IN-SOL	IN propylene glycol + Tween® 80 control solution
CS	chitosan chloride
SLN	solid lipid nanoparticles
NLC	nanostructured lipid carriers
SCR	Sclera-choroid-retinal pigment epithelium
IPBS	Isotonic phosphate buffered saline
HPβCD	Hydroxypropyl-beta-cyclodextrin
RMβCD	Randomly methylated beta-cyclodextrin
Alcohol	190-proof (“over proof”) / 95% Alcohol by volume (ABV).

References

1. Toker MI, et al. The effects of topical ketorolac and indomethacin on measles conjunctivitis: randomized controlled trial. Am J Ophthalmol. 2006; 141(5):902–905. [PubMed: 16527227]
2. Allegri P, et al. Randomized, double-blind, placebo-controlled clinical trial on the efficacy of 0.5% indomethacin eye drops in uveitic macular edema. Invest Ophthalmol Vis Sci. 2014; 55(3):1463–1470. [PubMed: 24519421]
3. Weber M, et al. Efficacy and safety of indomethacin 0.1% eye drops compared with ketorolac 0.5% eye drops in the management of ocular inflammation after cataract surgery. Acta Ophthalmol. 2013; 91(1):e15–e21. [PubMed: 22970738]
4. Botting RM. Inhibitors of cyclooxygenases: mechanisms, selectivity and uses. J Physiol Pharmacol. 2006; 57(Suppl 5):113–124.
5. Russo A, et al. Topical nonsteroidal anti-inflammatory drugs for macular edema. Mediators Inflamm. 2013; 2013:476525. [PubMed: 24227908]
6. Kern TS, et al. Topical administration of nepafenac inhibits diabetes-induced retinal microvascular disease and underlying abnormalities of retinal metabolism and physiology. Diabetes. 2007; 56(2): 373–379. [PubMed: 17259381]
7. Chetoni P, et al. Pharmacokinetics and anti-inflammatory activity in rabbits of a novel indomethacin ophthalmic solution. J Ocul Pharmacol Ther. 2000; 16(4):363–372. [PubMed: 10977132]

8. Kahanne LI, et al. Indosol--a nonsteroidal anti-inflammatory drug with therapeutic efficacy. Acta Pharm Hung. 1994; 64(4):125–129. [PubMed: 7976366]
9. Hippalgaonkar K, et al. Indomethacin-loaded solid lipid nanoparticles for ocular delivery: development, characterization, and in vitro evaluation. J Ocul Pharmacol Ther. 2013; 29(2):216–228. [PubMed: 23421502]
10. Patel A, et al. Ocular drug delivery systems: An overview. World J Pharmacol. 2013; 2(2):47–64. [PubMed: 25590022]
11. Cholkar K, et al. Novel Nanomicellar Formulation Approaches for Anterior and Posterior Segment Ocular Drug Delivery. Recent Pat Nanomed. 2012; 2(2):82–95. [PubMed: 25400717]
12. Fangueiro JF, et al. Ocular Drug Delivery - New Strategies for Targeting Anterior and Posterior Segments of the Eye. Curr Pharm Des. 2016; 22(9):1135–1146. [PubMed: 26675225]
13. Gaudana R, et al. Ocular drug delivery. AAPS J. 2010; 12(3):348–360. [PubMed: 20437123]
14. Morrison PW, Khutoryanskiy VV. Advances in ophthalmic drug delivery. Ther Deliv. 2014; 5(12): 1297–1315. [PubMed: 25531930]
15. Sultana Y, et al. Review of ocular drug delivery. Curr Drug Deliv. 2006; 3(2):207–217. [PubMed: 16611007]
16. Murugan K, et al. Parameters and characteristics governing cellular internalization and trans-barrier trafficking of nanostructures. Int J Nanomedicine. 2015; 10:2191–2206. [PubMed: 25834433]
17. Liu D, et al. Potential advantages of a novel chitosan-N-acetylcysteine surface modified nanostructured lipid carrier on the performance of ophthalmic delivery of curcumin. Sci Rep. 2016; 6:28796. [PubMed: 27350323]
18. Mainardes RM, et al. Colloidal carriers for ophthalmic drug delivery. Curr Drug Targets. 2005; 6(3):363–371. [PubMed: 15857294]
19. Khare, A., et al. Progress in Adhesion and Adhesives. John Wiley & Sons, Inc.; 2015. Mucoadhesive Polymers for Enhancing Retention in Ocular Drug Delivery; p. 451-484.
20. Ranaldi G, et al. The effect of chitosan and other polycations on tight junction permeability in the human intestinal Caco-2 cell line(1). J Nutr Biochem. 2002; 13(3):157–167. [PubMed: 11893480]
21. Caramella C, et al. Chitosan and its derivatives as drug penetration enhancers. Journal of Drug Delivery Science and Technology. 2010; 20(1):5–13.
22. Bonferoni MC, et al. Chitosan and its salts for mucosal and transmucosal delivery. Expert Opin Drug Deliv. 2009; 6(9):923–939. [PubMed: 19637983]
23. Uner M, Yener G. Importance of solid lipid nanoparticles (SLN) in various administration routes and future perspectives. Int J Nanomedicine. 2007; 2(3):289–300. [PubMed: 18019829]
24. Liu R, et al. Nanostructured lipid carriers as novel ophthalmic delivery system for mangiferin: improving in vivo ocular bioavailability. J Pharm Sci. 2012; 101(10):3833–3844. [PubMed: 22767401]
25. Jain-Vakkalagadda B, et al. Identification and functional characterization of a Na+-independent large neutral amino acid transporter, LAT1, in human and rabbit cornea. Invest Ophthalmol Vis Sci. 2003; 44(7):2919–2927. [PubMed: 12824232]
26. Tak RV, et al. Transport of acyclovir ester prodrugs through rabbit cornea and SIRC-rabbit corneal epithelial cell line. J Pharm Sci. 2001; 90(10):1505–1515. [PubMed: 11745709]
27. Majumdar S, et al. Transcorneal permeation of L- and D-aspartate ester prodrugs of acyclovir: delineation of passive diffusion versus transporter involvement. Pharm Res. 2009; 26(5):1261–1269. [PubMed: 18839288]
28. Vadlapudi AD, et al. Novel biotinylated lipid prodrugs of acyclovir for the treatment of herpetic keratitis (HK): transporter recognition, tissue stability and antiviral activity. Pharm Res. 2013; 30(8):2063–2076. [PubMed: 23657675]
29. Ahuja M, Dhake AS, Majumdar DK. Effect of formulation factors on in-vitro permeation of diclofenac from experimental and marketed aqueous eye drops through excised goat cornea. Yakugaku Zasshi. 2006; 126(12):1369–1375. [PubMed: 17139162]
30. Ahuja M, et al. Topical ocular delivery of NSAIDs. AAPS J. 2008; 10(2):229–241. [PubMed: 18437583]

31. Kim SJ, et al. Topical Nonsteroidal Anti-inflammatory Drugs and Cataract Surgery: A Report by the American Academy of Ophthalmology. Ophthalmology. 2015; 122(11):2159–2168. [PubMed: 26123091]
32. Tres F, et al. Indomethacin-Kollidon VA64 Extrudates: A Mechanistic Study of pH-Dependent Controlled Release. Mol Pharm. 2016; 13(3):1166–1175. [PubMed: 26845251]
33. Bahl D, Bogner RH. Amorphization alone does not account for the enhancement of solubility of drug co-ground with silicate: the case of indomethacin. AAPS Pharm Sci Tech. 2008; 9(1):146–153.
34. McMillan J, Batrakova E, Gendelman HE. Cell delivery of therapeutic nanoparticles. Prog Mol Biol Transl Sci. 2011; 104:563–601. [PubMed: 22093229]
35. Almeida H, et al. Nanoparticles in Ocular Drug Delivery Systems for Topical Administration: Promises and Challenges. Curr Pharm Des. 2015; 21(36):5212–5224. [PubMed: 26412360]
36. Battaglia L, et al. Application of lipid nanoparticles to ocular drug delivery. Expert Opin Drug Deliv. 2016:1–15.
37. Chime SA, Onyishi IV. Lipid-based drug delivery systems (LDDS): Recent advances and applications of lipids in drug delivery. African Journal of Pharmacy and Pharmacology. 2013; 7(48):3034–3059.
38. Uner M. Preparation, characterization and physico-chemical properties of solid lipid nanoparticles (SLN) and nanostructured lipid carriers (NLC): their benefits as colloidal drug carrier systems. Pharmazie. 2006; 61(5):375–386. [PubMed: 16724531]
39. De Campos AM, et al. The effect of a PEG versus a chitosan coating on the interaction of drug colloidal carriers with the ocular mucosa. Eur J Pharm Sci. 2003; 20(1):73–81. [PubMed: 13678795]
40. de la Fuente M, Seijo B, Alonso MJ. Novel hyaluronic acid-chitosan nanoparticles for ocular gene therapy. Invest Ophthalmol Vis Sci. 2008; 49(5):2016–2024. [PubMed: 18436835]
41. Vllasaliu D, et al. Tight junction modulation by chitosan nanoparticles: comparison with chitosan solution. Int J Pharm. 2010; 400(1–2):183–193. [PubMed: 20727955]
42. de Campos AM, et al. Chitosan nanoparticles as new ocular drug delivery systems: in vitro stability, in vivo fate, and cellular toxicity. Pharm Res. 2004; 21(5):803–810. [PubMed: 15180338]
43. Gukasyan, JH., Kim, K-J., Lee, HLV. The Conjunctival Barrier in Ocular Drug Delivery. In: Ehrhardt, C., Kim, K-J., editors. Drug Absorption Studies: In Situ, In Vitro and In Silico Models. Boston MA: Springer US; 2008. p. 307-320.
44. He J, et al. Preparation, Pharmacokinetics and Body Distribution of Silymarin-Loaded Solid Lipid Nanoparticles After Oral Administration. Journal of Biomedical Nanotechnology. 2007; 3(2):195–202.
45. Manjunath K, Venkateswarlu V. Pharmacokinetics, tissue distribution and bioavailability of nitrendipine solid lipid nanoparticles after intravenous and intraduodenal administration. J Drug Target. 2006; 14(9):632–645. [PubMed: 17090399]
46. Mei D, et al. Effect of chitosan structure properties and molecular weight on the intranasal absorption of tetramethylpyrazine phosphate in rats. Eur J Pharm Biopharm. 2008; 70(3):874–881. [PubMed: 18656537]
47. Verheul RJ, et al. Influence of the degree of acetylation on the enzymatic degradation and in vitro biological properties of trimethylated chitosans. Biomaterials. 2009; 30(18):3129–3135. [PubMed: 19339046]
48. Dale O, et al. Transepithelial transport of morphine and mannitol in Caco-2 cells: the influence of chitosans of different molecular weights and degrees of acetylation. J Pharm Pharmacol. 2006; 58(7):909–915. [PubMed: 16805950]
49. Al-Halafi AM. Nanocarriers of nanotechnology in retinal diseases. Saudi J Ophthalmol. 2014; 28(4):304–309. [PubMed: 25473348]
50. Barar J, et al. Ocular Drug Delivery; Impact of in vitro Cell Culture Models. J Ophthalmic Vis Res. 2009; 4(4):238–252. [PubMed: 23198080]
51. Thassu, D., Chader, GJ. Ocular drug delivery systems: barriers and application of nanoparticulate systems. CRC Press; 2012.

52. Liu CH, et al. Novel lutein loaded lipid nanoparticles on porcine corneal distribution. J Ophthalmol. 2014; 2014:304694. [PubMed: 25101172]

53. Castelli F, et al. Characterization of indomethacin-loaded lipid nanoparticles by differential scanning calorimetry. International Journal of Pharmaceutics. 2005; 304(1–2):231–238. [PubMed: 16188405]

54. Bucolo C, et al. Ocular pharmacokinetics profile of different indomethacin topical formulations. J Ocul Pharmacol Ther. 2011; 27(6):571–576. [PubMed: 22059858]

55. Klang S, Abdulrazik M, Benita S. Influence of emulsion droplet surface charge on indomethacin ocular tissue distribution. Pharm Dev Technol. 2000; 5(4):521–532. [PubMed: 11109251]

56. Yamaguchi M, et al. Mucoadhesive properties of chitosan-coated ophthalmic lipid emulsion containing indomethacin in tear fluid. Biol Pharm Bull. 2009; 32(7):1266–1271. [PubMed: 19571396]

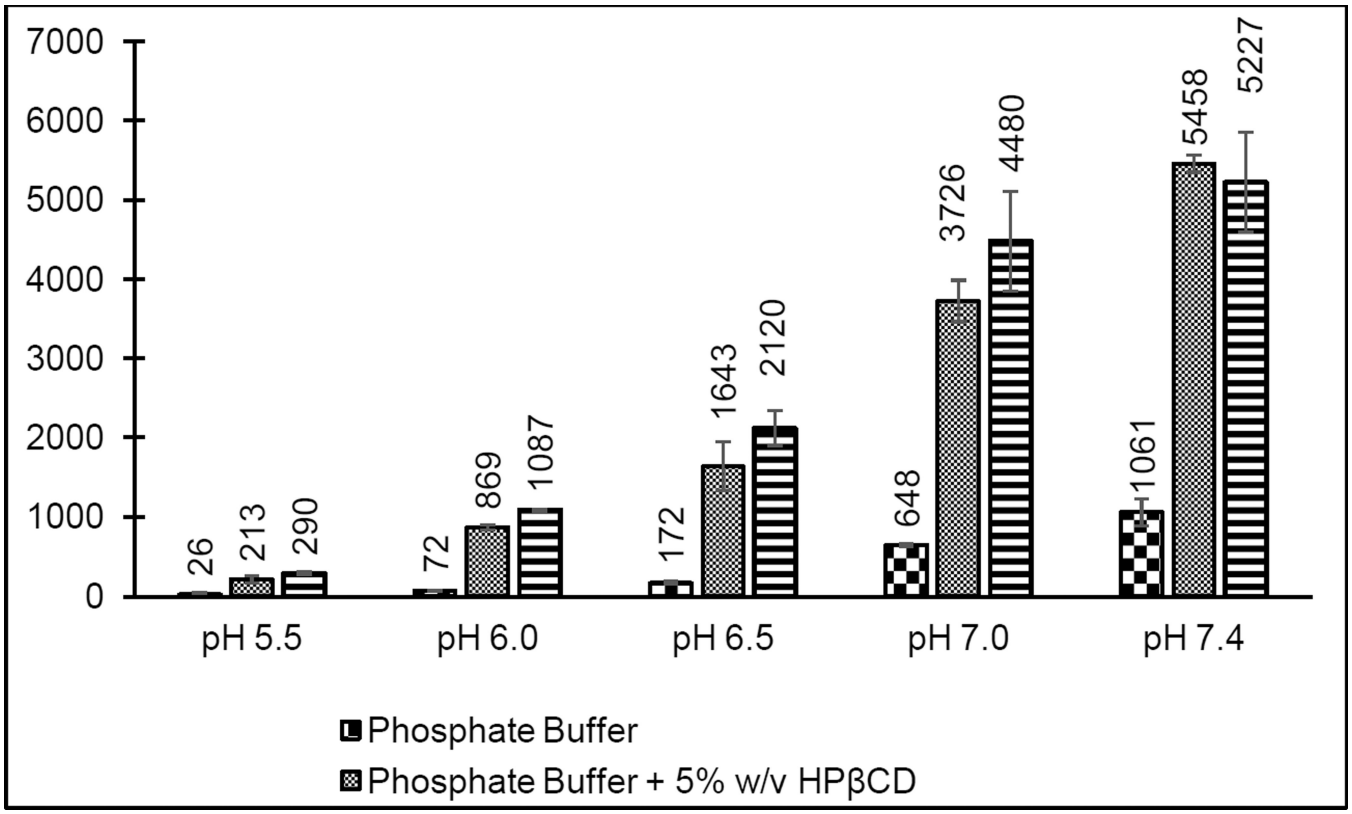

Figure 1.

pH-dependent saturation solubility of IN in phosphate buffer, 5% w/v HPβCD in phosphate buffer, and 5% w/v RMβCD in phosphate buffer (μg/mL). The results are depicted as the mean ± SD (n=3).

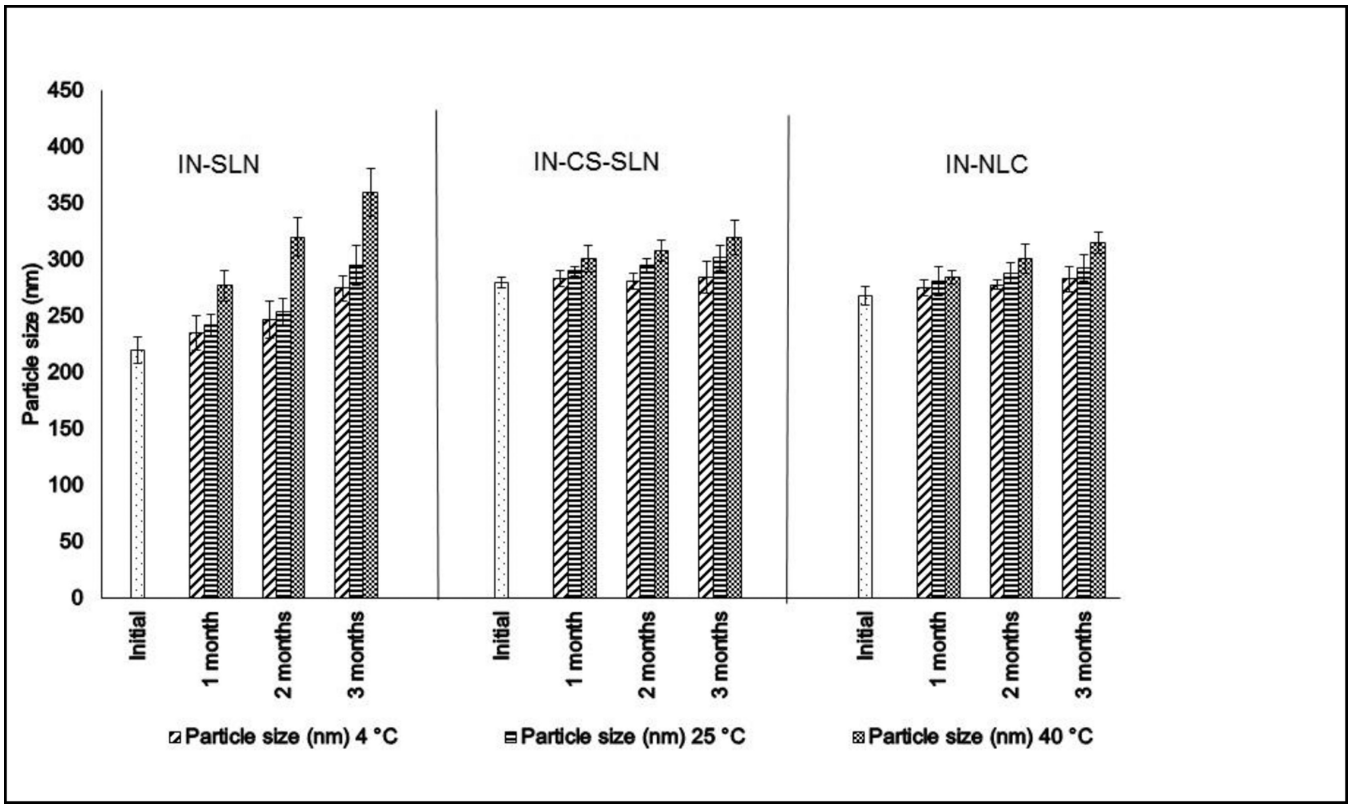

Figure 2.

Particle size characteristics of various IN formulations following storage at 4°C, 25°C/60% RH, and 40°C/75% RH. The data represent the mean ± S.D (n=3).

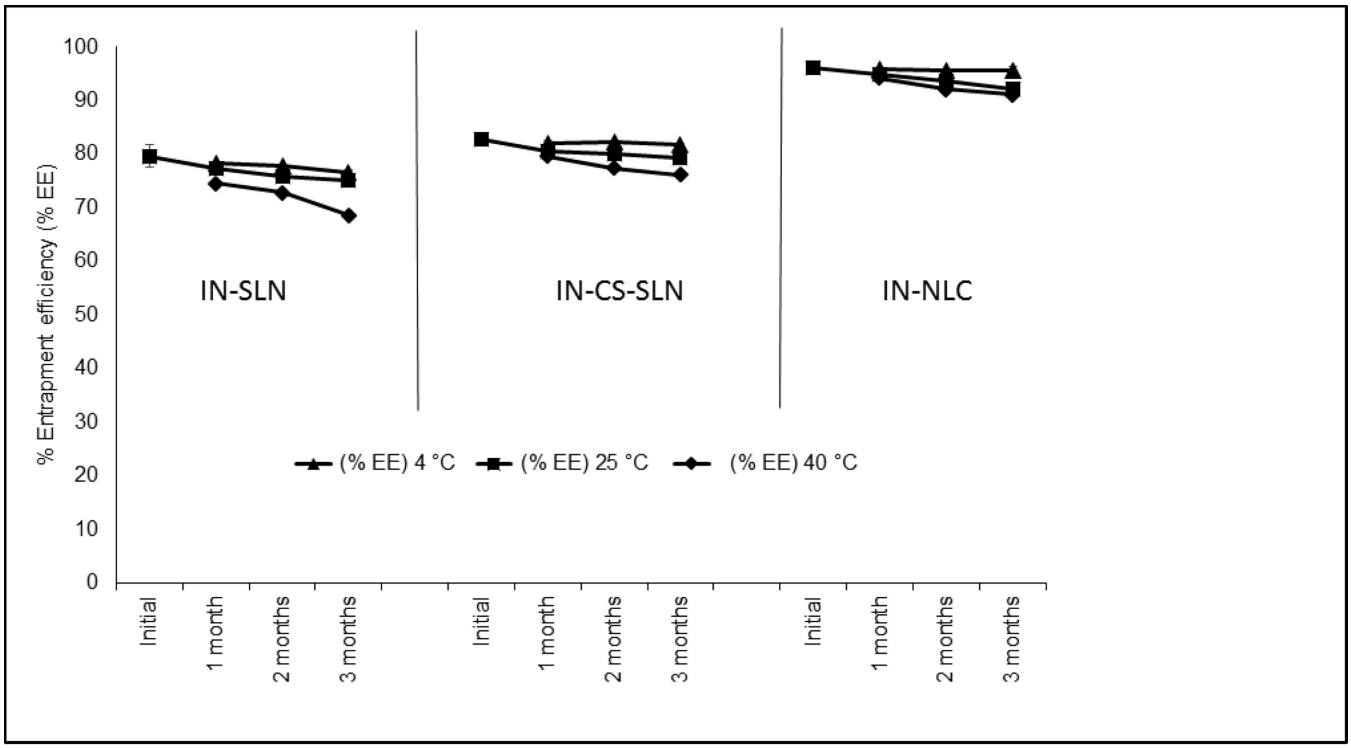

A:

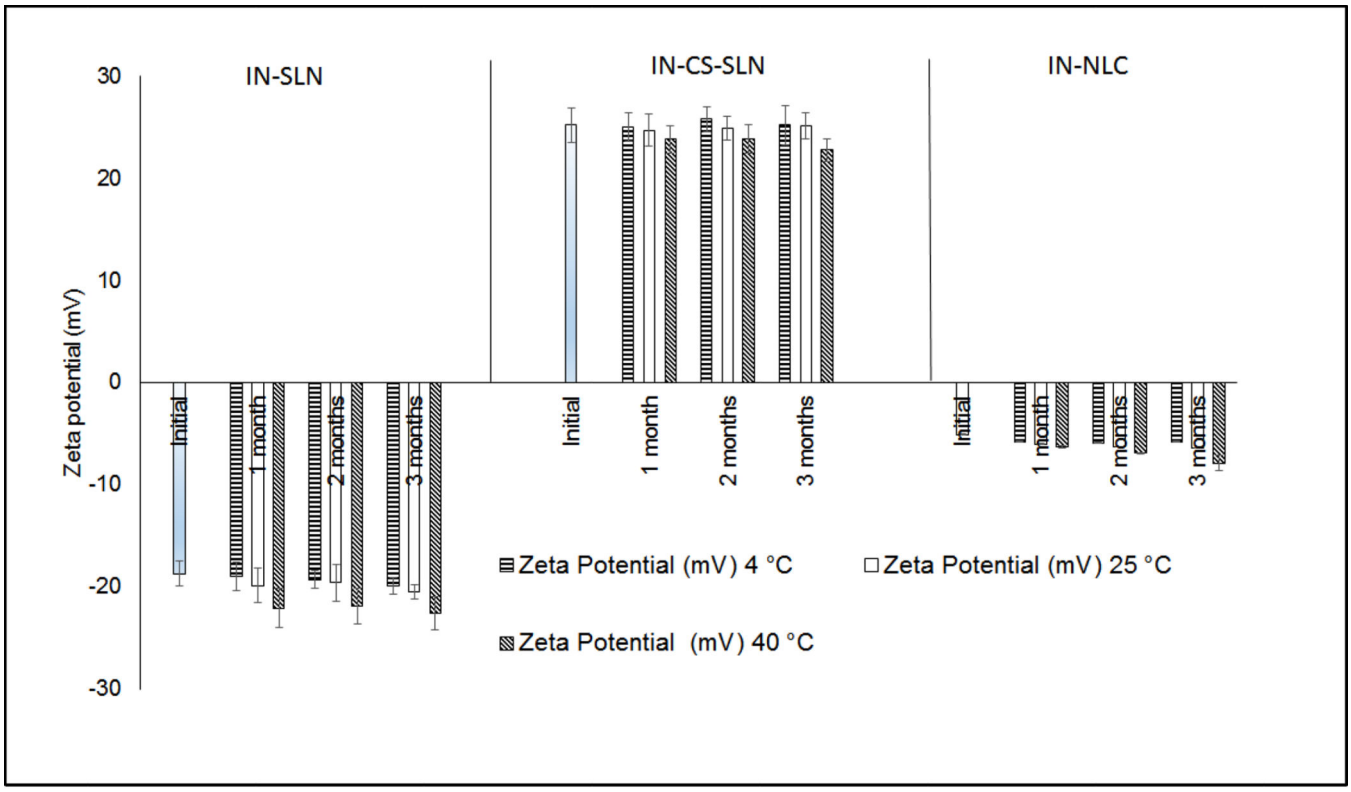

B:

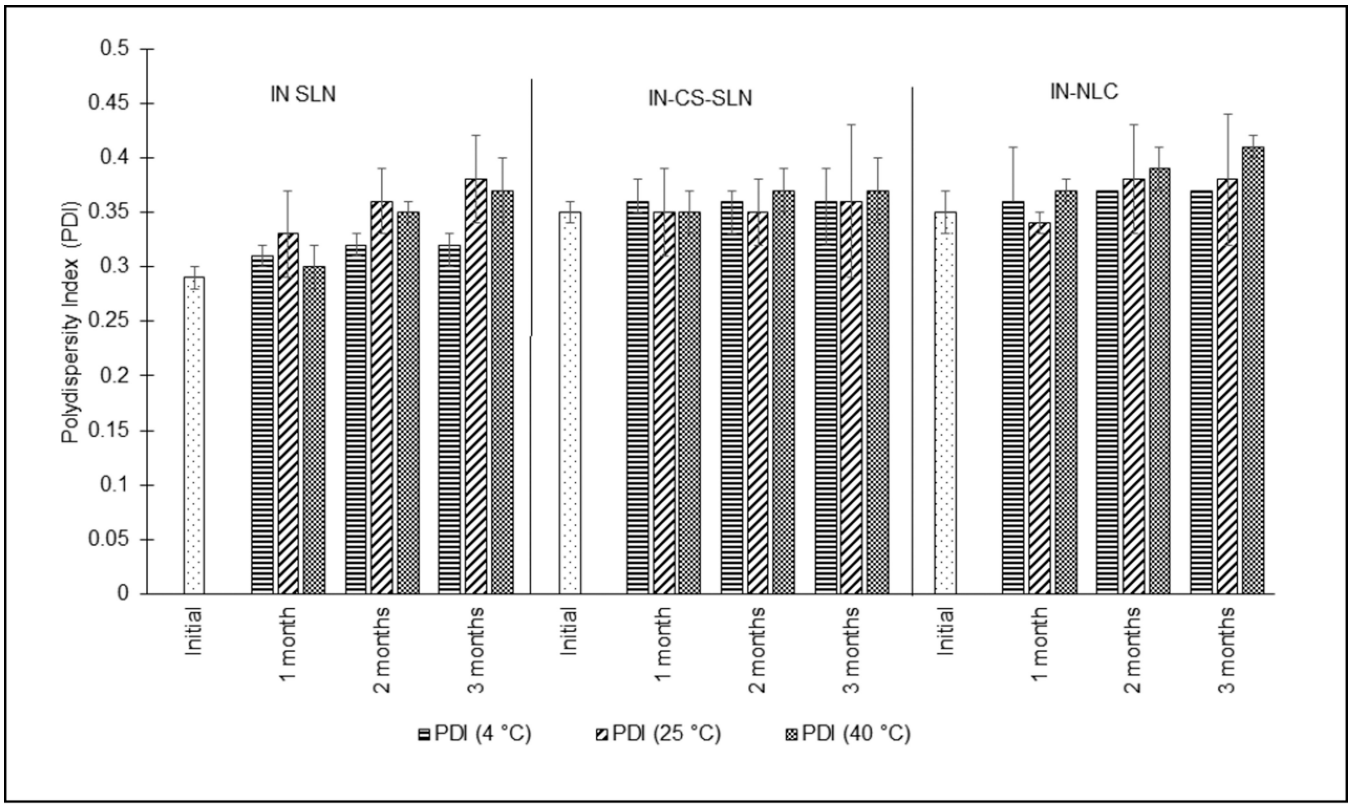

C:

Figure 3.

A: Entrapment efficiency (% EE) of various IN formulations following storage at 4°C, 25°C/60% RH, and 40°C/75% RH. The data represent the mean ± S.D (n=3).

B: Zeta potential of various IN formulations following storage at 4°C, 25°C/60% RH, and 40°C/75% RH. The data represent the mean ± S.D (n=3).

C: Polydispersity indices (PDI) of various IN formulations following storage at 4°C, 25°C/60% RH, and 40°C/75% RH. The data represent the mean ± S.D (n=3).

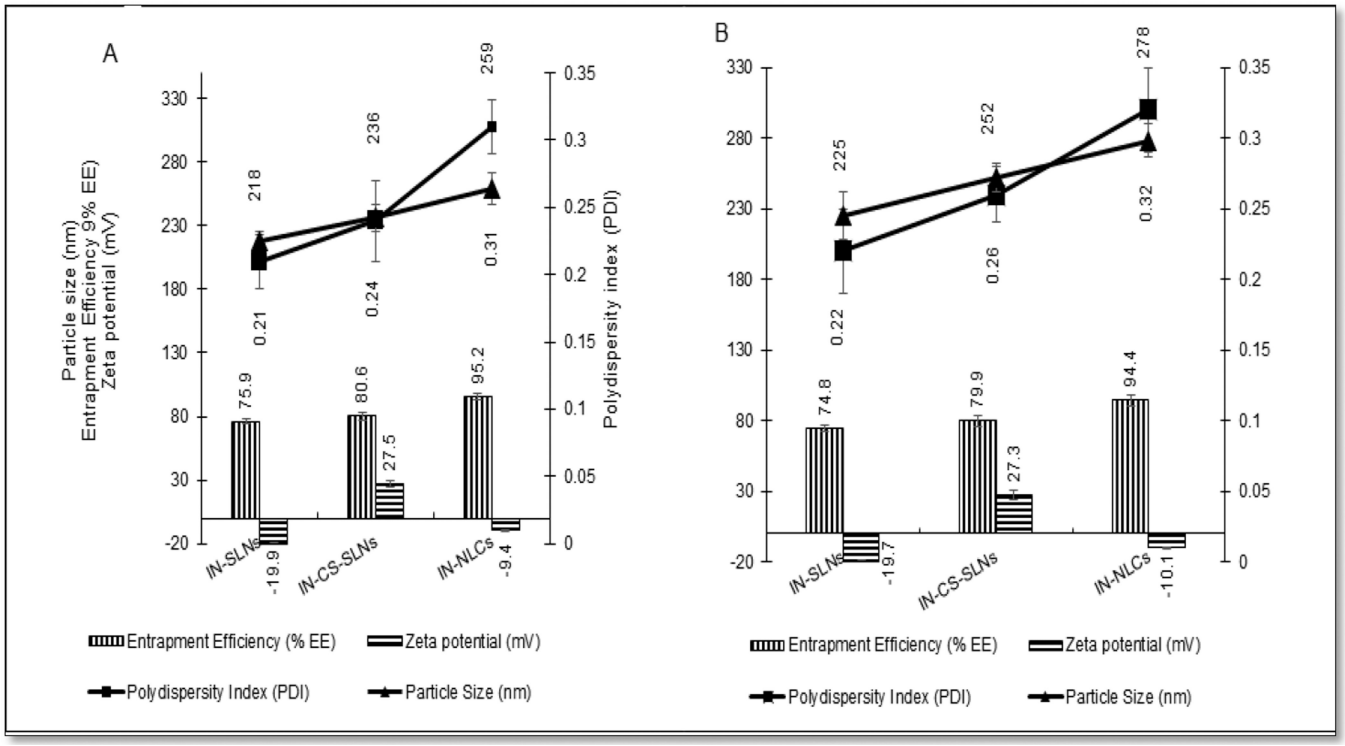

Figure 4.

Physico-chemical characteristics of the IN SLN and NLC formulations pre-sterilization (Fig 4A) and post-sterilization (4B). The data represent the mean ± S.D (n=3).

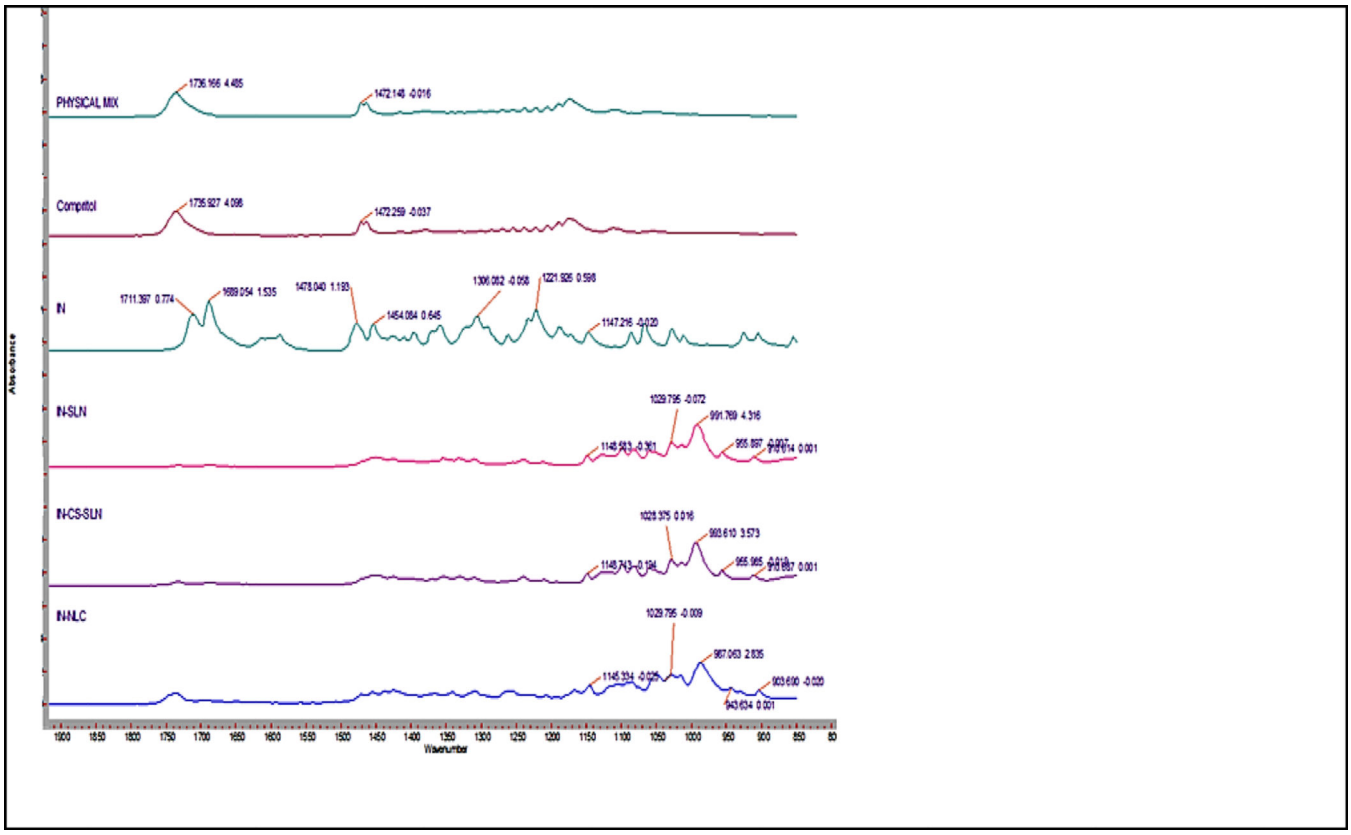

Figure 5.
FTIR spectral images of the IN + Compritol physical mixture, Compritol, IN, IN-SLN, IN-CS-SLN and IN-NLC F-1 formulations.

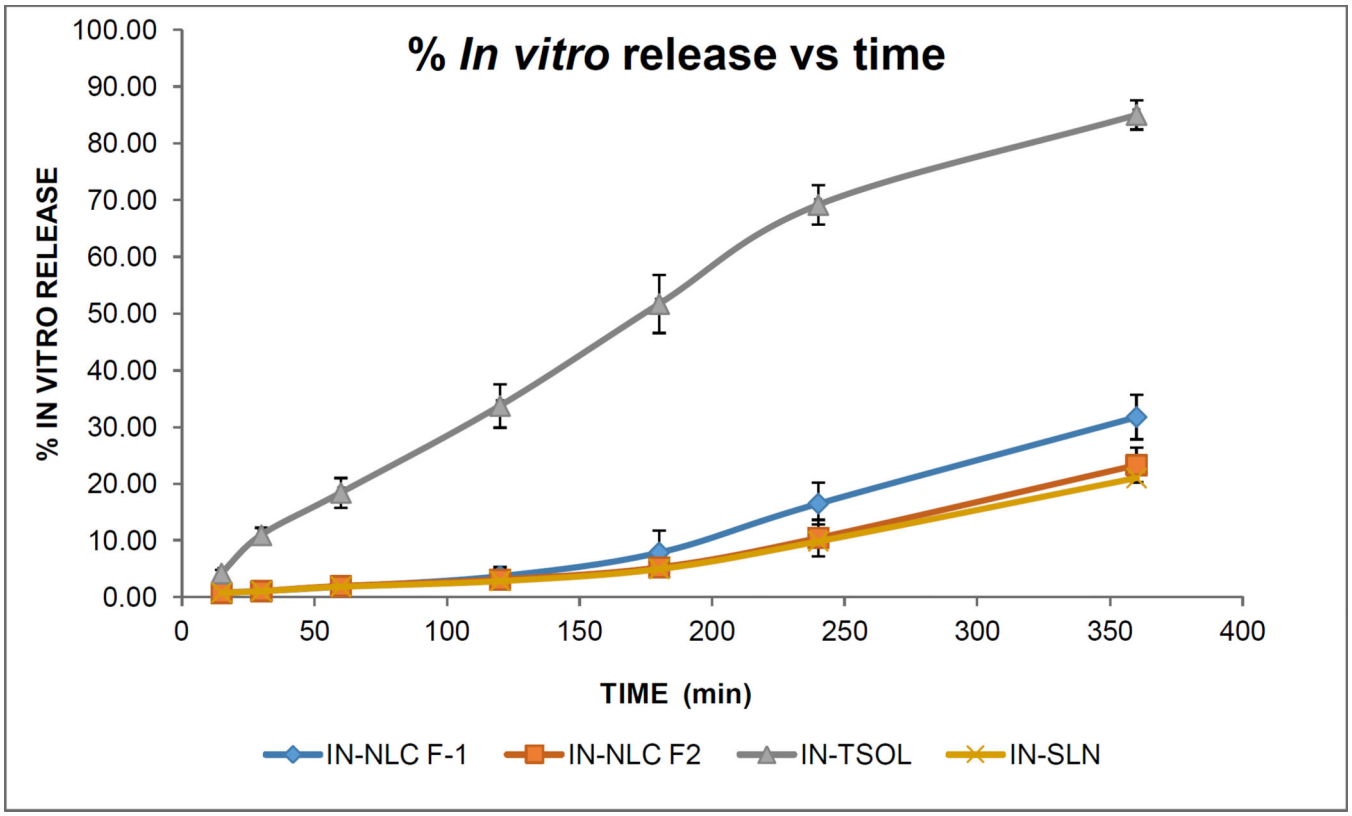

Figure 6.

In vitro release of IN from various formulations across Spectra/Por® membranes at 34°C. Receiver solution consisted of IPBS containing 2.5% w/v RMβCD (pH 7.4). The results are depicted as the mean ± S.D (n=3).

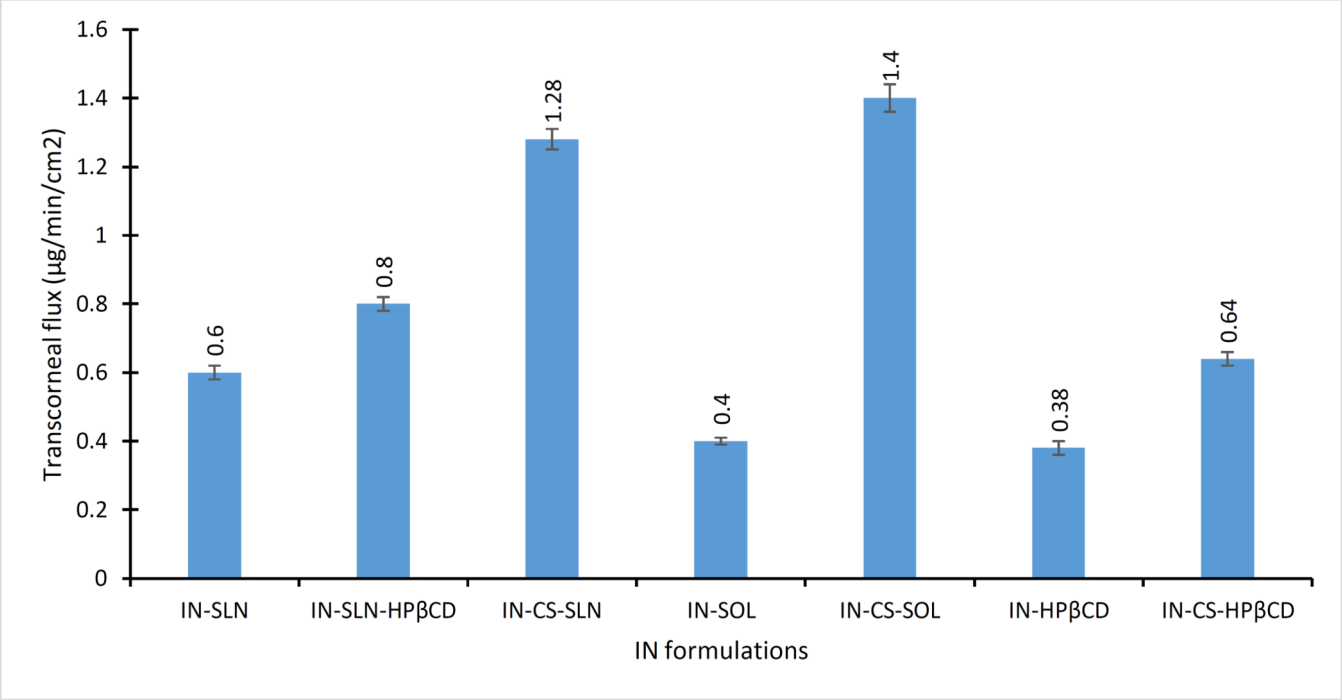

Figure 7.

Transcorneal flux across isolated rabbit cornea from various IN topical formulations at 34°C. The receiver solution consisted of IPBS containing 2.5% w/v RMβCD (pH 7.4). The results are depicted as the mean ± S.D (n=4).

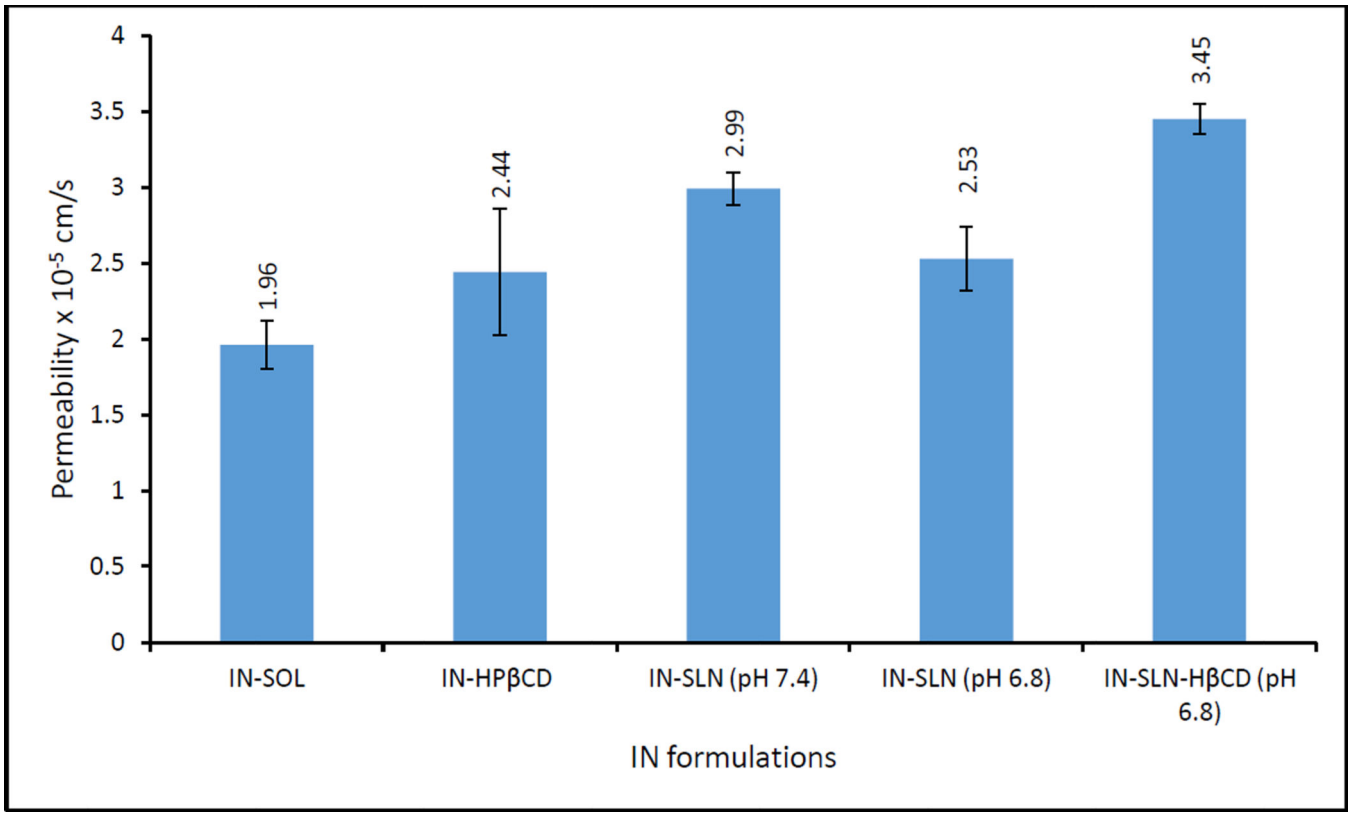

Figure 8.

Trans-SCR permeability of IN from various topical ocular formulations at 34°C. The receiver solution consisted of IPBS containing 2.5% w/v RMβCD (pH 7.4). The results are depicted as the mean ± S.D (n=3).

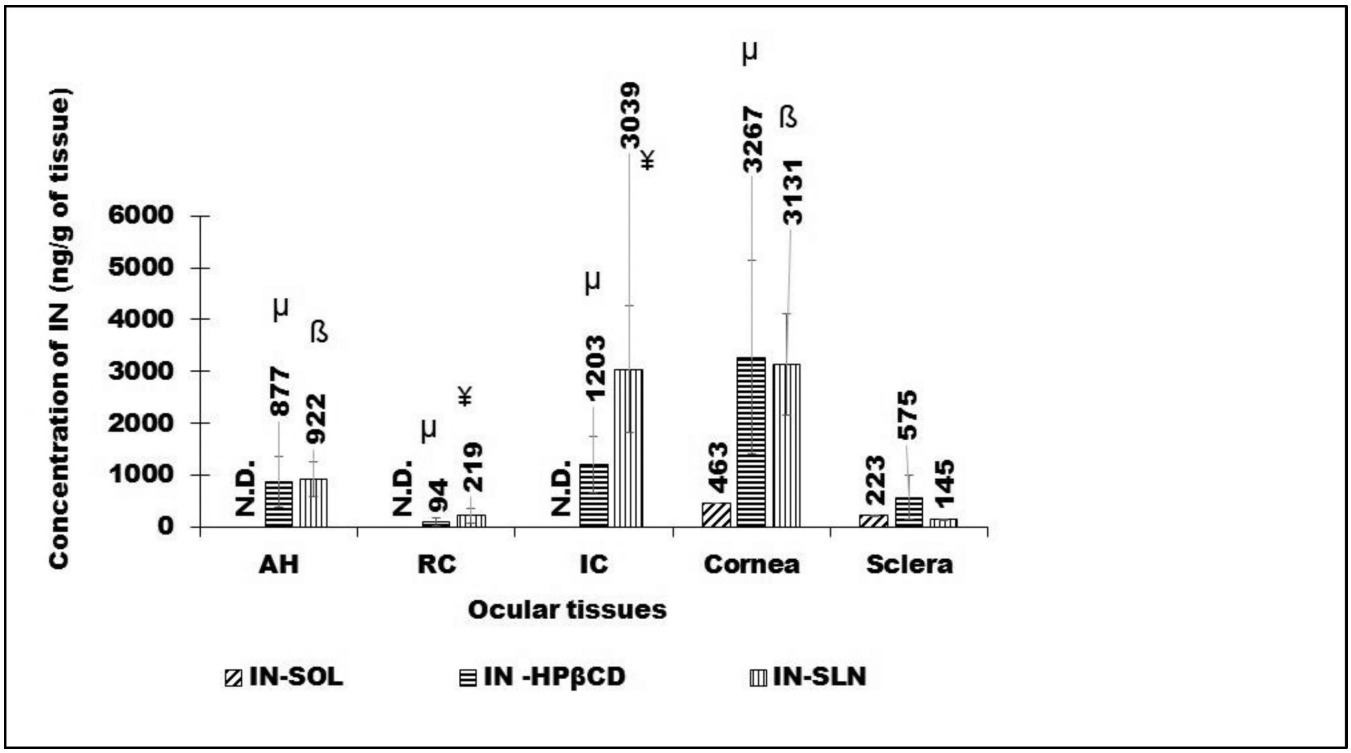

Figure 9.

IN ocular tissue concentrations (ng/g of tissue) obtained from the IN-SOL, IN-HPβCD, and IN-SLN formulations 2 hrs post-topical administration in the anesthetized rabbit model. The data represent the mean ± S.D. (n=3). AH: Aqueous humor; VH: Vitreous humor; IC: Iris-Ciliary; RC: Retina-Choroid. (N.D., not detected). Different symbols, such as μ and β, indicate significant differences ($p<0.05$) of the IN-HPβCD and IN-SLN formulations compared to IN-SOL. ¥ represents a significant difference in the ocular tissue concentrations of IN for use of the IN-SLNs compared to all other formulations.

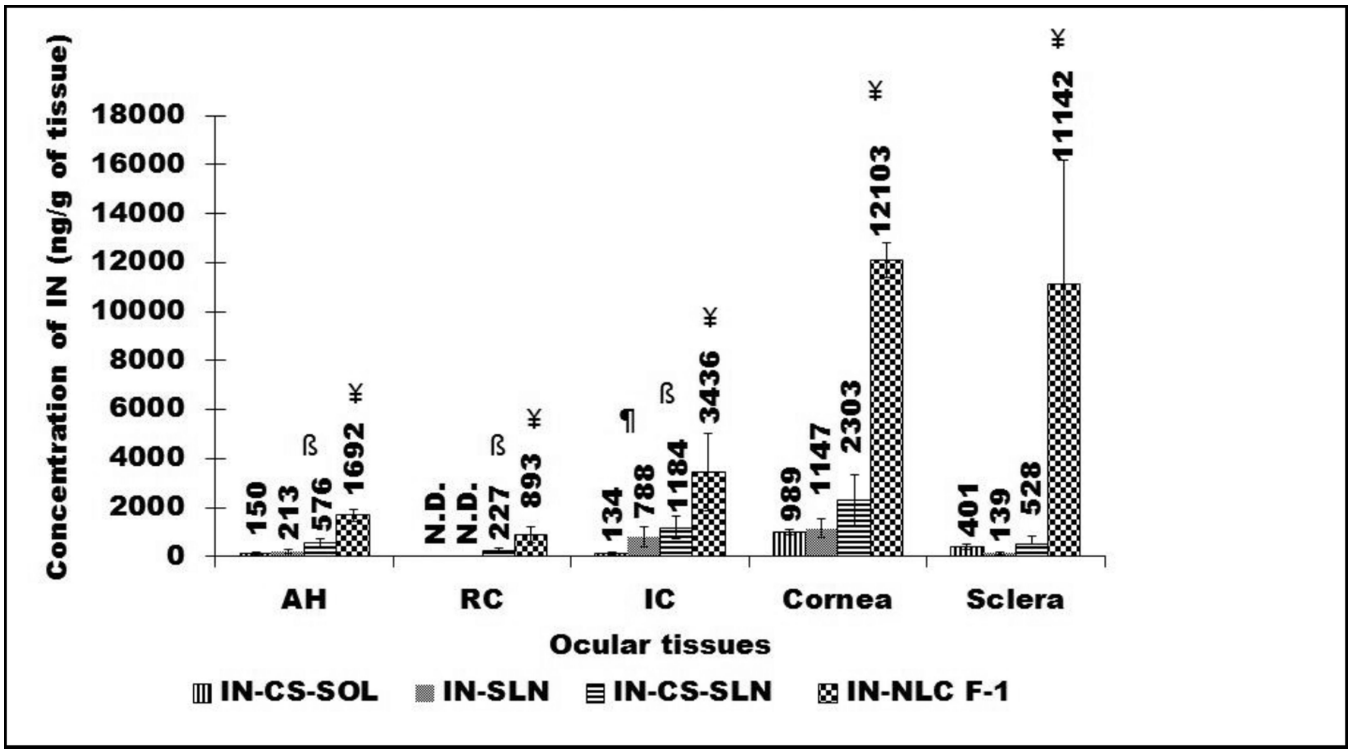

Figure 10.

IN ocular tissue concentrations (ng/gm of tissue) obtained from the IN-CS-SOL, IN-SLN, IN-CS-SLN (n=6) and IN-NLC formulations 2 hrs post-topical administration in the conscious rabbit model. The data represent the mean ± S.D. All the experiments were performed in triplicate if not indicated otherwise. Different symbols, such as ¶ and β, indicate significant differences ($p<0.05$) of the IN-SLN and IN-CS-SLN formulations compared to IN-CS-SOL. ¥ represents a significant difference in the ocular tissue concentrations of IN for use of the IN-NLCs compared to all other formulations.

Table 1

Composition of IN formulations with individual components represented by weight (mg).

Formulation composition	IN formulations							
	IN-TSOL	IN-SOL	IN-CS-SOL	IN-HPBCD	IN-SLN-HPβCD	IN-SLN	IN-CS-SLN	F-1 IN-NLC
IN (mg)	10	10	10	10	10	10	10	80
Compritol (mg)	-	-	-	-	200	200	200	260
Miglyol® 812	-	-	-	-	-	-	-	140
Poloxamer 188 (mg)	-	-	-	-	25	25	25	25
Tween® 80 (mg)	100	100	100	-	75	75	75	75
Glycerin (mg)	-	-	-	-	225	225	225	225
Propylene glycol (mg)	-	2930	2930	-	-	-	-	-
CS (mg)	-	-	10	-	-	-	25	-
HPβCD (mg)	-	-	-	250	250	-	-	-
Water (mL)	10	10	10	10	10	10	10	10

Table 2

Composition of lipid mixtures used in the NLC formulations. The particle size characteristics, PDI, zeta potential, entrapment efficiency and assay values for each formulation are presented below.

IN-NLC formulations	F-1	F-2	F-3	F-4	F-5	F-6
IN (0.8% w/v)	80	80	80	80	80	80
Compritol (60%)	240	240	240	240	240	240
Miglyol 812 (40%)	160	-	320	640	-	-
Miglyol 829 (40%)	-	160	-	-	320	640
Total lipid (%; mg)	4%; 400	4%; 400	8%; 800	16%; 1600	8%; 800	16%; 1600
particle size (nm)	227	279.1	304.1	519.2	385.1	629.1
Polydispersity index (PDI)	0.235	0.259	0.433	0.58	0.456	0.381
Zeta potential (mV)	−12.2	−5.57	−0.92	0.027	−2.58	−0.304
Entrapment efficiency (%) EE	99.8	99.74	100	100	100	99.9
Assay (%)	96.8	97.8	97.4	91.3	96.2	92.5